Lab on a Chip

Cite this: DOI: 10.1039/c2lc20800h

www.rsc.org/loc

PAPER

A microfluidic device for high throughput bacterial biofilm studies†

Jeongyun Kim,‡[a] Manjunath Hegde,‡[a] Sun Ho Kim,[b] Thomas K. Wood[a] and Arul Jayaraman*[a]

Received 23rd August 2011, Accepted 20th January 2012
DOI: 10.1039/c2lc20800h

Bacteria are almost always found in ecological niches as matrix-encased, surface-associated, multi-species communities known as biofilms. It is well established that soluble chemical signals produced by the bacteria influence the organization and structure of the biofilm; therefore, there is significant interest in understanding how different chemical signals are coordinately utilized for community development. Conventional methods for investigating biofilm formation such as macro-scale flow cells are low-throughput, require large volumes, and do not allow spatial and temporal control of biofilm community formation. Here, we describe the development of a PDMS-based two-layer microfluidic flow cell (μFC) device for investigating bacterial biofilm formation and organization in response to different concentrations of soluble signals. The μFC device contains eight separate microchambers for cultivating biofilms exposed to eight different concentrations of signals through a single diffusive mixing-based concentration gradient generator. The presence of pneumatic valves and a separate cell seeding port that is independent from gradient-mixing channels offers complete isolation of the biofilm microchamber from the gradient mixer, and also performs well under continuous, batch or semi-batch conditions. We demonstrate the utility of the μFC by studying the effect of different concentrations of indole-like biofilm signals (7-hydroxyindole and isatin), either individually or in combination, on biofilm development of pathogenic *E. coli*. This model can be used for developing a fundamental understanding of events leading to bacterial attachment to surfaces that are important in infections and chemicals that influence the biofilm formation or inhibition.

1.0 Introduction

Bacteria form biofilms by adhering to surfaces and developing complex communities called biofilms,[1] in which multicellular aggregates of cells are encased in an extracellular polymeric matrix.[2,3] Biofilms impact humans in many ways as they can form in natural, medical, and industrial settings. For example, formation of biofilms on medical devices, such as catheters or implants often result in difficult-to-treat chronic infections.[4] Inside the human body, biofilms are naturally found in the oral cavity[5] and in the gastrointestinal (GI) tract,[6] where a large number of non-pathogenic (commensal or probiotic) bacterial species exist and help in normal host functions (*e.g.*, food digestion, immune system development, protection from exogenous pathogens).[7] When ecological shifts occur within the *in vivo* microbial community, it results in diseases such as periodontal disease in the oral cavity[8] or ulcerative colitis in the GI tract.[9]

Cell-cell communication through chemical signals such as autoinducer-2 (AI-2),[10] acyl homoserine lactones (AHLs),[11] and indole[12] has been shown to play a role in the development and sustenance of biofilm communities.[13,14] Work from our laboratory has shown that indole, which is formed during the breakdown of tryptophan by the tryptophanase enzyme and is secreted in nearly 27 genera[12] including those present in the GI tract (*e.g.*, *Bacteroides thetaiotaomicron*,[15] *Escherichia coli*[16]), decreases the formation of *E. coli* biofilms[12,17] and increases *Pseudomonas aeruginosa* biofilm formation.[12] In *E. coli*, indole is secreted at high concentrations (600 μM per ~10^9 cells) when grown in rich medium[18] and has been detected in human feces at comparable concentrations (~250–1100 μM).[19,20] The relevance of indole in the context of the GI tract is evident from our prior work showing that indole counters enterohaemorrhagic *E. coli* (EHEC) O157:H7 infections, as it repels the pathogen, decreases motility and adherence to epithelial cells, downregulates the expression of genes related to virulence and infection, and decreases its biofilm formation.[17] Indole can also be transformed to derivatives such as 2-hydroxyindole, 3-hydroxyindole, 4-hydroxyindole, 7-hydroxyindole, isatin (indole-2,3,-dione), indigo, isoindigo, and indirubin[21] by oxygenases in strains such as *Pseudomonas putida* PpG7,[22] *Ralstonia picketti* PK01,[23] *Pseudomonas mendocina* KR,[24] *Burkholderia cepacia* G4.[21] Since bacterial communities contain multiple species with a wide-range

[a]*Department of Chemical Engineering, Texas A&M University, 222 Jack E. Brown Engineering Building, 3122 TAMU, College Station, TX, 77843-3122. E-mail: arulj@tamu.edu; Fax: (+1) 979 845 6446; Tel: (+1) 979 845 3306*
[b]*Department of Pediatrics, Massachusetts General Hospital, Boston, MA, 02114*

† Electronic supplementary information (ESI) available. See DOI: 10.1039/c2lc20800h

‡ These authors contributed equally to this work.

of biotransformation capabilities, it is highly likely that derivatives of signals such as indole are also likely to be present in bacterial communities.[18] Work from our lab has also shown that hydroxyindoles and isatin also impact biofilm formation.[17,25] Although, indole and 7-hydroxyindole (7-HI) inhibit *E. coli* biofilm formation,[12,25] isatin increases biofilm formation.[25] Intriguingly indole and 7-HI both promote *P. aeruginosa* biofilm formation[12,25] (while dramatically reducing virulence[26]), suggesting that the same signal can be used by different bacterial species in a markedly different manner, and motivate the need for investigating the effect of a broad range of signals on biofilm formation dynamics.

Conventional formats for investigating biofilm formation under conditions of shear utilize macro-scale flow cells in which the biofilm is formed on a glass slide and fresh medium or a dilute cell suspension is continuously perfused through the system.[27] While widely used, this system has the obvious disadvantages of requiring large volumes (limiting when using signals or molecules that are not readily available), is not suited for high-throughput investigation, and does not facilitate spatial and temporal control of biofilm formation. Microfluidic models for biofilm studies have been recently proposed;[28–31] however, currently available models are either low-throughput[30,31] or require expensive instrumentation and lack flexibility.[28]

In this work, we describe the development of a microfluidic biofilm model that contains eight separate microchambers for cultivating biofilms exposed to eight different concentrations of signals through a single gradient mixer (high-throughput) and is fully customizable. The incorporation of pneumatic valves and a separate cell seeding port that is independent from gradient-mixing channels offers the ability to operate the device under flow, batch or semi-batch conditions. We demonstrate the utility of this microfluidic biofilm model by investigating the concentration-dependent interaction between different bacterial signals (7-hydroxyindole and isatin) on EHEC biofilm formation.

2.0 Materials and methods

2.1 Bacterial strains, materials and growth media

E. coli O157:H7 (CDC EDL933; referred to as EHEC) was obtained from the American Type Culture Collection (ATCC 43895, Manassas, VA, USA). The EHEC isogenic mutant deficient in indole (Δ*tnaA*) was constructed in the lab using the method of Wanner and Datsenko.[32] Plasmid pCM18[33] was used to constitutively express the green fluorescent protein (GFP) in EHEC, and erythromycin (150 μg mL^{-1}) was used for maintaining pCM18 in EHEC. Isatin, indole, and 7-HI were obtained in powdered form from Thermo Fisher Scientific (New Jersey, USA). EHEC strains were seeded in M9 minimal medium[34] supplemented with 0.2% glucose for attachment to glass surfaces in biofilm experiments. Routine culture and biofilm development (*i.e.*, after seeding) was carried out in Luria Bertani broth (LB; 10 g L^{-1} tryptone, 10 g L^{-1} NaCl, 5 g L^{-1} yeast extract).

2.2 Microdevice design, fabrication, and characterization

The PDMS-based μFC device (Fig. 1) was fabricated in the Materials Characterization Facility at Texas A&M University using soft lithographic techniques.[35] The μFC device consists of a glass cover slip and two PDMS layers - a bottom layer with a diffusive-mixer and eight microchambers and a top layer which contains the pneumatic elements for opening and closing microvalves that separate the diffusive mixer and bacteria seeding ports from the microchambers. The top layer also contains a bacterial seeding port for introducing bacteria into the microchambers. The diffusive gradient-mixer in the bottom layer was used to generate different concentrations of 7-HI or isatin and to perfuse growth media into the microchambers. The dimension of the diffusive mixer was 200 μm (width) × 200 μm (height) and the biofilm microchambers were 8000 μm (length) × 600 μm (width) × 200 μm (height). All pneumatic channels were 200 μm thick. The two PDMS layers were fabricated separately and assembled by sequential oxygen plasma treatment and bonding (oxygen gas flow rate of 10 sccm, 100 W, 40 s) in a plasma etcher. The top pneumatic layer membrane was first aligned and bonded to the bottom diffusive-mixer/microchamber layer, followed by bonding of the combined PDMS layer to a cover glass (22 × 50 mm) while applying vacuum through the pneumatic ports. Tygon tubing (0.01″ ID × 0.03″ OD, Saint Gobain performance plastics, OH, USA) was used for all fluidic connections. Two PicoPlus 11 syringe pumps (Harvard Apparatus, MA, USA) were used to separately control fluid flow rates in the two layers. A temperature controlled metal slide holder was used to maintain the temperature of the device at 37 °C. Moist air flowed continuously over the device in order to maintain humidity and avoid bubble formation inside the microchambers. The opening and closing of valves were pneumatically controlled by introducing vacuum or compressed air. Generation of the desired concentration range in the device was verified by forming a gradient of fluorescein isothiocyanate (FITC) ranging from 0–1 mM at a flow rate of 2 μL min^{-1} and quantifying the concentration of FITC in each chamber using fluorescence microscopy and image analysis.

2.3 Biofilm development in microfluidic devices

An overnight culture of EHEC grown in LB at 37 °C was washed and resuspended in M9-glucose (minimal) media at a turbidity at 600 nm of ~1.0 as cells resuspended in minimal media attached better to glass than cells in nutrient-rich media (Hegde and Jayaraman, unpublished results). The bacterial suspension was introduced into the eight biofilm microchambers through the cell inlet (Fig. 1). During this process, the main inlet valves (Fig. 2A) remained closed to prevent cells from entering and attaching to the gradient mixing channels (which would disrupt mixing in the channels). The main outlet valves and seeding valves were then closed, and the culture was maintained without flow for 2 h to promote attachment of bacteria to the glass surface. After 2 h, the main inlet and outlet valves were opened (Fig. 2B), and unattached cells were removed by perfusing nutrient rich LB media at a flow rate of 2 μL min^{-1}. The attached bacteria were allowed to form biofilm at 37 °C by flowing LB and LB supplemented with a specific concentration of a specific signal (*i.e.*, 7-HI or isatin) through the two inlets of the diffusive mixer into the microchambers at a flow rate of 2 μL min^{-1} for 8 h. For individual treatments, 7-HI concentrations across the eight microchambers were 0, 71, 143, 214, 286, 357, 429, and 500 μM and isatin concentrations were 0, 29, 57, 86, 114, 143, 171, and 200 μM. 7-HI

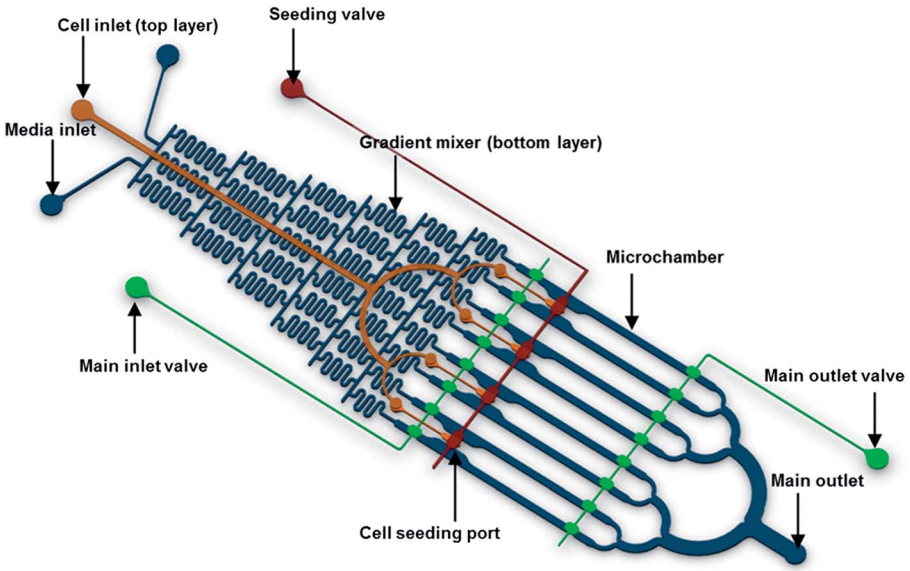

Fig. 1 Microfluidic flow cell (μFC) for studying bacterial biofilms. The device consists of a glass cover slip and two PDMS layers - a bottom layer with a diffusive-mixer and eight microchambers and a top layer with the pneumatic elements for opening and closing microvalves that separate the diffusive mixer and bacteria seeding ports from the microchambers. The top layer also contains a bacterial seeding port for introducing bacteria into the microchambers.

and isatin were cytotoxic beyond 1000 μM and 250 μM, respectively. Hence concentrations used were below this range.

2.4 Confocal microscopy and biofilm quantitation

Images were taken on a TCS SP5 scanning confocal laser microscope (Leica Microsystems, Wetzlar, Germany) using a 40X/0.85 NA dry objective. Z-stack images were acquired at a zoom level of 2.2 such that the image covered 100% of width of the microchamber. Two individual positions per microchamber covering a total of 70% of the microchamber length were chosen for imaging. 3-D reconstruction of the biofilm architecture was performed using IMARIS 3D and 4D Real-Time Interactive Data Visualization software (Bitplane Inc., CT, USA).

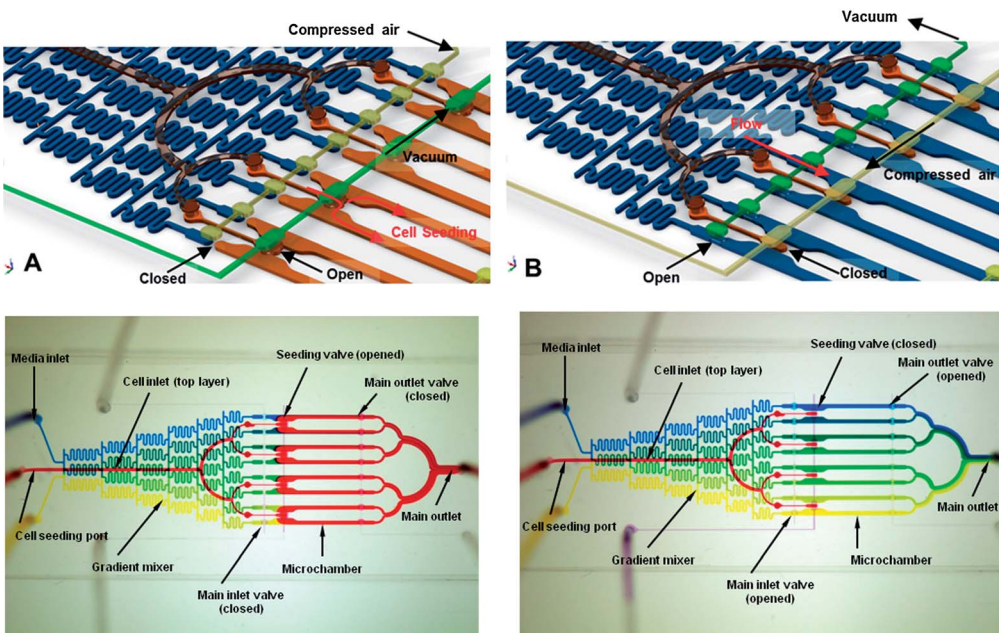

Fig. 2 Bacterial seeding and exposure to exposure to signaling molecules. (**A**) During cell seeding into the microchambers, the seeding valve is opened and main inlet and outlet valves are closed to prevent back flow of cells into the gradient mixer. Top panel shows a schematic of the cell seeding process. Bottom panel shows red dye in the microchambers introduced through the cell seeding port, with the blue-to-yellow concentration gradient excluded from the microchambers. (**B**) During biofilm development in the microchamber and exposure to signals, the seeding valve is closed and the main inlet and outlet valves are opened for the culture media to flow through the microchamber. Top panel shows a schematic of the signaling molecule exposure step. Bottom panel shows the blue-to-yellow color gradient in the microchambers, with the red dye in the cell seeding port excluded.

Biomass and average biofilm height were obtained using the COMSTAT, a MATLAB-based image-processing script developed by Heydorn *et al.*[36] Briefly, thresholding of the image stacks was performed by applying a fixed threshold value (a value between 0 and 255 determined by the user), followed by a segmentation process called connected-volume filtration, in which the layer of biomass at the substratum is used as starting point and the algorithm moves down the stack of images determining which pixels are connected to the pixels in the layer below, hence eliminating all the noise on or after the images. The number of pixels associated with the biofilm (ONE) and the background (ZERO) was calculated from each image in the Z-stack and combined to obtain the bio-volume or biomass, thickness distribution, and the average thickness of the biofilm. Z-stack images were acquired from two individual positions in each microchamber per experiment and data obtained from three such independent experiments were used to calculate the average and one standard deviation of biomass and biofilm thickness as shown in Tables 1 and 2. Statistical significance was determined at a significance level of $p < 0.05$ using an independent *t*-test.

3.0 Results and discussion

3.1 Operation of the μFC device

The aim of this study was to develop a microfluidic flow cell (μFC) device for high-throughput biofilm formation studies. The μFC device consisted of a glass slide and two PDMS layers, a bottom layer with a diffusive mixer[37,38] and eight microchambers, and a top layer which contains the pneumatic elements for controlling microvalves (Fig. 1). The eight microchambers were used for developing bacterial biofilms and exposing them to eight concentrations of soluble signals generated on-chip in the gradient-mixer. Eight different concentrations of individual signals or combination of multiple signaling molecules can be generated on-chip in the diffusive mixer. Since absorption of molecules into PDMS is well established,[39] a concentration gradient of 0–1 mM FITC was generated and maintained for 12 h to ensure that a linear concentration gradient was established across the eight microchambers (Supplemental Fig. S1†).

For seeding cells in the device, bacteria were introduced through the cell inlet in the top layer and the connected cell seeding port in the bottom layer into each microchamber. During this operation the main inlet valves were closed by applying compressed air and seeding valves were opened by applying vacuum (Fig. 2A). The main inlet valves connecting the gradient-mixer and microchamber were closed to prevent cells seeded into the microchamber from entering the gradient mixer channels. After seeding cells into the microchamber, all three valves (main inlet, main outlet, and seeding valves) remained closed so that cells attached to the glass surface without flow (*i.e.*, under batch conditions). After attachment of bacteria for 2 h, the inlet and outlet valves were opened by applying vacuum (Fig. 2B) and unattached or loosely attached bacteria were removed by flowing culture media. Biofilms were allowed to form and develop by perfusing media containing different concentrations of signaling molecule(s) into the microchambers.

The μFC model offers significant advantages over conventional macroscale biofilm models and previously developed microfluidic models. First, this model enables simultaneous investigation of the effect of a range of concentrations of a single signal or combinations of multiple signals on EHEC biofilm formation, which precluded the use of previously described microfluidic flow cells.[28–31] For example, the micro flow cell design used by Lee *et al.*[31] to study *Staphylcoccus epidermidis* biofilms contains a single channel with multiple inlets, which makes it difficult for studying the effect of different concentrations on biofilm organization as the gradient is created across a single channel. Also, since the design utilizes the same port for cell seeding and flowing nutrient media, it is possible that the plastic tubes supplying media can get clogged and disrupts the flow dynamics. In our μFC device, the cell seeding port is distinct from the nutrient media port, which minimizes any clogging of the device. However, due to the possibility of residual cells colonizing the seeding channel and tubing, it is not possible to reuse the device for multiple experiments. The design used by Cho *et al.*[29] to study the self-organization of *E. coli* colonies into biofilms, and Kim *et al.*[30] to study the effect of a gradient of antibiotics on *P. aeruginosa* biofilms have constraints similar to the device described by Lee *et al.*[31] The design proposed by Benoit *et al.*[28] eliminates the use of tubes, and thereby, prevents

Table 1 COMSTAT analysis showing the variation in average EHEC biofilm height and biomass in LB at 37 °C upon 8 h exposure to (i) a 0–500 μM gradient of 7-HI, (ii) a 0–200 μM gradient of isatin. Data with one standard deviation shown are from three experiments and two positions per microchamber per experiment

	7-HI (0–500 μM)			Isatin (0–200 μM)		
Microchamber	Concentration (μM)	Average Biofilm Height (μm)	Biomass ($\mu m^3\ \mu m^{-2}$)	Concentration (μM)	Average Biofilm Height (μm)	Biomass ($\mu m^3\ \mu m^{-2}$)
1	0	4.2 ± 0.7	3.8 ± 0.4	0	5.6 ± 0.9	4.4 ± 0.4
2	71	3.7 ± 0.5	3.4 ± 0.4	29	6.9 ± 0.4	5.6 ± 0.4
3	143	3.1 ± 0.5	2.5 ± 0.3	57	7.4 ± 0.5	6.2 ± 0.3
4	214	1.9 ± 0.6[a]	1.7 ± 0.2[a]	86	10.2 ± 1.3	8.8 ± 0.2
5	286	0.6 ± 0.1[a]	0.41 ± 0.03[a]	114	12.1 ± 0.8[a]	10.1 ± 0.7[a]
6	357	0.12 ± 0.04[a]	0.09 ± 0.03[a]	143	11.9 ± 0.6[a]	9.8 ± 0.7[a]
7	429	0.07 ± 0.05[a]	0.03 ± 0.02[a]	171	12.6 ± 0.3[a]	10.7 ± 0.3[a]
8	500	0.03 ± 0.01[a]	0.02 ± 0.01[a]	200	13.3 ± 0.6[a]	11.2 ± 0.4[a]

[a] indicates a statistically-significant ($p < 0.05$) change relative to microchamber 1.

Table 2 COMSTAT analysis showing the variation in average EHEC biofilm height and biomass in LB at 37 °C upon 8 h exposure to (i) competing gradients of 7-HI and isatin (*i.e.*, 500 μM 7-HI and 200 μM isatin introduced with LB through the same media inlet and plain LB introduced through the other inlet) (ii) cross-mixed gradient of 7-HI and isatin (*i.e.*, 500 μM 7-HI and 200 μM isatin introduced with LB through two different inlets). Data from microchamber 1 for competing gradients (No 7-HI and isatin treatment) was used as a control for comparing the effect of 7-HI and/or isatin on EHEC biofilm. Data with one standard deviation shown are from three experiments and two positions per microchamber per experiment

	Competing gradient 7-HI (0–500 μM) + Isatin (0–200 μM)				Cross-mixed gradient 7-HI (0–500 μM) + Isatin (200 μM-0)			
Microchamber	7-HI (μM)	Isatin (μM)	Average Biofilm Height (μm)	Biomass ($\mu m^3\ \mu m^{-2}$)	7-HI (μM)	Isatin (μM)	Average Biofilm Height (μm)	Biomass ($\mu m^3\ \mu m^{-2}$)
1	0	0	4.8 ± 0.5	4.0 ± 0.4	0	200	8.6 ± 0.8	6.3 ± 0.4
2	71	29	4.5 ± 0.5	3.9 ± 0.4	71	171	6.3 ± 0.2	4.8 ± 0.4
3	143	57	4.3 ± 0.3	3.6 ± 0.3	143	143	5.6 ± 0.4	4.1 ± 0.3
4	214	86	3.7 ± 0.6	3.3 ± 0.2	214	114	3.8 ± 0.6[a]	2.6 ± 0.5[a]
5	286	114	3.3 ± 0.4	2.5 ± 0.4	286	86	3.1 ± 0.3[a]	1.9 ± 0.4[a]
6	357	143	2.7 ± 0.7	2.1 ± 0.6[a]	357	57	2.2 ± 0.3[a]	1.1 ± 0.4[a]
7	429	171	2.1 ± 0.4[a]	1.8 ± 0.2[a]	429	29	1.3 ± 0.4[a]	0.06 ± 0.03[a]
8	500	200	1.2 ± 0.3[a]	1.1 ± 0.3[a]	500	0	0.07 ± 0.02[a]	0.03 ± 0.01[a]

[a] indicates a statistically-significant ($p < 0.05$) change relative to microchamber 1.

biofouling and is amenable to high-throughput studies (simultaneous operation of 24 reactors). However, it is not customizable and any manipulation of signal concentration needs to be performed manually, whereas the generation of different concentration ranges is performed through the diffusive mixer[37,38] on-chip in our device.

Although PDMS is known to absorb small molecules,[39] it is unlikely that the concentration in the different microchambers was significantly different from the predicted concentrations for the duration of our experiments. This is because the μFC device was operated as a continuous flow system, and medium containing a fixed concentration of the signal of interest (*e.g.*, isatin) was flowed through each PDMS channel continuously. While absorption of chemical molecules could occur initially, it is likely that the PDMS was saturated rapidly due to the continuous replenishment of signal; thereby, maintaining the desired concentration in each microchamber. This is demonstrated in Supplemental Fig. S1 where no appreciable change in the FITC concentration profile is observed in all the microchambers over 12 h (*i.e.*, the duration of the biofilm experiments) and no residual FITC was detected after rinsing the microchambers for 5 min.† It should also be noted that the concentration gradient used in our studies was broad (0–250 or 500 μM) and the effects of small changes in the signal concentration on biofilm formation were not observed; however, it is possible that absorption causes changes in the biological response when lower concentrations or narrower concentration ranges are used.

3.2 Effect of range of concentrations of 7-HI and isatin on EHEC biofilm

Our lab previously demonstrated that indole and 7-HI inhibit EHEC biofilm development, but isatin, which is also a derivative of indole, promotes biofilm formation.[25] However, these studies only investigated the effect of each signaling molecule at a single concentration (*e.g.* 1000 μM for 7-HI and 250 μM for isatin) due to the use of macro-scale flow cells. Since derivatives of signals can be present in the biofilm microenvironment at a wide range of concentrations, we used the μFC device to investigate the effect of a range of concentrations of 7-HI and isatin on EHEC biofilm in a single experiment.

We tested the effect of eight equally distributed concentrations of 7-HI ranging from 0 (microchamber 1) to 500 μM (microchamber 8) on EHEC biofilm in LB medium, as EHEC forms robust biofilms in LB medium[25] at 37 °C. After 8 h, EHEC formed a biofilm with an average height of 4.2 ± 0.7 μm and biomass of 3.8 ± 0.4 $\mu m^3\ \mu m^{-2}$ in control microchambers (*i.e.*, not exposed to 7-HI; microchamber 1 in Fig. 3A). When exposed to concentrations between zero and 357 μM 7-HI, the biofilm height and biomass decreased linearly with increasing concentration of 7-HI (Table 1). The biofilm thickness and biomass formed in microchamber 6 containing 357 μM of 7-HI was ~35- and ~42-fold, respectively, less than that observed in microchamber 1. No significant biofilm was formed in microchambers 7 and 8 containing 7-HI concentrations above 357 μM (Fig. 3A and Table 1). Thus 7-HI concentrations above ~350 μM completely inhibit *E. coli* biofilm formation.

Unlike 7-HI, exposure to isatin increased the formation of EHEC biofilms (Fig. 3B and Table 1). The increase in both biofilm thickness and biomass levels was linear in the 0–200 μM range, with microchamber 1 (no isatin) having a biofilm thickness of 5.6 ± 0.9 μm and biomass of 4.4 ± 0.4 $\mu m^3\ \mu m^{-2}$, and microchamber 8 (200 μM isatin) having a thickness of 13.3 ± 0.6 μm and biomass of 11.2 ± 0.4 $\mu m^3\ \mu m^{-2}$. These results are consistent with data from prior studies[25] generated using macro-scale flow cells and demonstrate the validity of the μFC model. In addition, the ability to screen the effect of eight different signal concentrations in a single experiment demonstrates its suitability for high-throughput biofilm studies. It should be noted that while the current prototype allows investigation of biofilm formation under eight conditions simultaneously, it can be easily scaled to 12 to 16 concentrations based on the size of the prototype that can fit a single 50 by 22 mm glass slide.

The decrease in EHEC biofilm with increasing 7-HI concentrations could be due to an increase in the levels of cysteine, as 7-hydroxyindole regulates the cysteine synthesis operon (*cysADEIJP*),[25] and overproduces CysB, which positively regulates the biosynthesis of cysteine in *E. coli*,[40] and decreases EHEC biofilm formation.[25] In addition, 7-HI was also less potent in

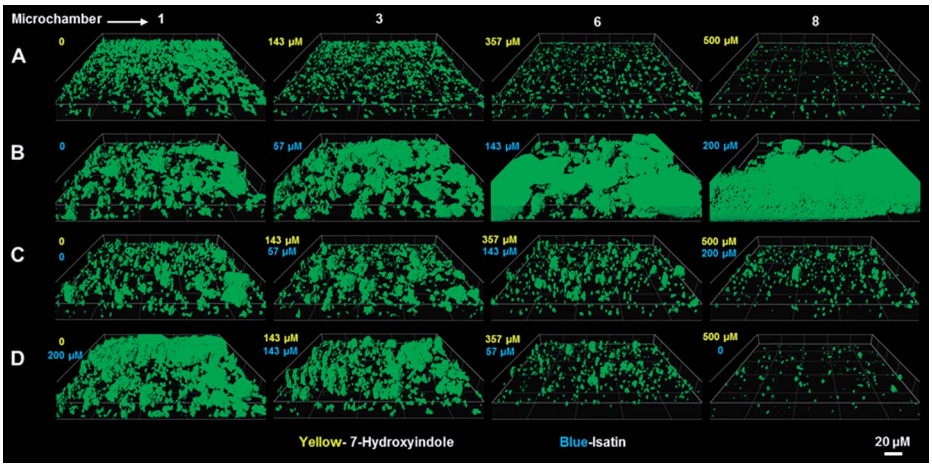

Fig. 3 Effect of 7-HI and isatin on EHEC biofilm formation. IMARIS representation of EHEC biofilm architecture in microchambers 1, 3, 6, and 8 of the μFC after 8 h exposure to (A) 7-HI (0–500 μM), (B) Isatin (0–200 μM), (C) 7-HI (500 μM) and isatin (200 μM) introduced through same inlet, and (D) 7-HI (500 μM) and isatin (200 μM) introduced through two different inlets. The concentration of 7-HI and isatin the chambers are shown in yellow and blue, respectively.

reducing EHEC biofilm formation in the absence of cysteine.[25] The effect of isatin on EHEC biofilm could possibly be mediated through the AI-2 quorum sensing molecule. Isatin up-regulates the AI-2 transport genes (*lsrABCDFGKR*), and exposure to isatin likely increases the uptake of AI-2 inside the cell.[25] Since AI-2 also increases EHEC biofilm formation[25] like it does to K-12,[41] the increase in EHEC biofilm formation with increasing concentrations of isatin could be related to increased AI-2 activity.

3.3 Effect of combinations of 7-HI and isatin on EHEC biofilm formation

In addition to high-throughput investigations of biofilm formation, a second advantage of the microfluidic biofilm model is that it enables interrogation of the interaction between different signals on biofilm formation in a high-throughput manner. This is ecologically and physiologically relevant as biofilms are rarely present as mono-cultures in natural environments or *in vivo*[5,7,9] and the different signals present may exert divergent effects on bacterial physiology. For example, the indole produced by bacteria such as *E. coli* can be further modified (*e.g.*, through oxidation, hydroxylation, *etc.*) by other bacteria in the community, which, in turn, can lead to a diverse range of modified signals (*i.e.*, indole-like signals) being present in the biofilm microenvironment.[12] As shown in Fig. 3B and in our prior work,[12,25] not all indole derivatives exert the same effect on biofilm formation, as 7-HI and isatin can both be generated in a bacterial community from indole, and yet, they can exert divergent effects on EHEC biofilm formation. Thus, any bacterial species capable of carrying out biotransformation reactions with indole, irrespective of whether they themselves produce indole or not, can deplete the parent signal and produce different derivatives, and thereby, alter the extent of biofilm formation. More importantly, since the type of derivative formed and the concentration at which it is present varies depending on the biosynthetic capability of the microbial community, the observed effect on biofilm formation can vary widely. Therefore, we used the microfluidic biofilm model to investigate the effect of simultaneous exposure (*i.e.*, combination gradient) to 7-HI and isatin on EHEC biofilm formation.

Two types of combination gradients were generated in diffusive mixers as signals can be introduced in two ways into the diffusive mixer. The first is a competing gradient, which is formed when 7-HI and isatin are both introduced through the same inlet and media without any signals is introduced through the other inlet. This allows investigation of the effect that each signal, at different concentrations, has on biofilm formation in the presence of increasing levels of the other signal. The second, a cross-mixed gradient, is formed when signals are introduced through different inlets and the resultant gradient enables investigation of the effect of increasing levels of each signal in the presence of decreasing levels of the other signal on biofilm formation.

Using competing gradients, where the concentrations of 7-HI and isatin increased simultaneously across the eight chambers from 0–500 μM and 0–200 μM respectively, we found that when both the signals were present in concentrations similar in orders of magnitude, EHEC biofilm decreases (Table 2, Fig. 3C). This suggests that the effect of 7-HI on EHEC biofilm formation was more dominant than the effect of isatin at these concentrations. Using cross-mixed gradients, where the concentrations of 7-HI increased from 0–500 μM and isatin decreased from 200–0 μM across the eight chambers, we found that when the concentration of isatin was equal to or greater than that of 7-HI, EHEC biofilm increased (Table 2, panels 1 and 2 in Fig. 3D) compared to untreated control (panel 1, Fig. 3C). This indicated that isatin is more dominant when it is present at an equal or higher concentration compared to 7-HI. But, when the 7-HI concentration in the cross-mixed gradient exceeded the isatin concentration (panel 3 and 4, Fig. 3D), 7-HI was more dominant than isatin, and the biomass and height of the EHEC biofilm decreased (Table 2, Fig. 3C and 3D). Thus, if the isatin concentration exceeds that of 7-HI, EHEC biofilm increases and if the concentration of 7-HI exceeds that of isatin (in both competing and cross-mixed gradients), EHEC biofilm decreases.

4.0 Summary

Since antibiotic treatments are not effective in complete removal of bacterial biofilms formed by pathogens,[42] alternative strategies are needed to treat bacterial biofilms. We have developed a microfluidic device for investigating the effect of a wide range of concentrations of a single soluble signal or combinations of two or more signals on bacterial biofilm formation. This device enables screening of compounds and their concentrations that effectively inhibit biofilm formation of pathogenic bacteria. We have utilized this device to demonstrate that increasing concentrations of the biofilm signals, 7-HI and isatin, inhibit and stimulate EHEC biofilm formation respectively. We envision this device being used to investigate synergistic effects between multiple inhibitors on biofilm formation as a first step towards discovering low concentration biofilm inhibitory cocktails.

Acknowledgements

This work was supported by grants from the National Institutes of Health (R01 GM089999) to TKW and AJ and the National Science Foundation (CBET 0846453) to AJ. We thank Dr Tarun Bansal for constructing the EHEC Δ*tnaA* mutant used in this study.

References

1 J. W. Costerton, Z. Lewandowski, D. E. Caldwell, D. R. Korber and H. M. Lappin-Scott, *Annu. Rev. Microbiol.*, 1995, **49**, 711–745.
2 L. Hall-Stoodley and P. Stoodley, *Cell. Microbiol.*, 2009, **11**, 1034–1043.
3 C. Beloin, A. Roux and J. M. Ghigo, in *Bacterial Biofilms*, Springer Berlin Heidelberg, 2008, vol. 322, pp. 249–289.
4 L. Hall-Stoodley, J. W. Costerton and P. Stoodley, *Nat. Rev. Microbiol.*, 2004, **2**, 95–108.
5 P. E. Kolenbrander, R. J. Palmer, S. Periasamy and N. S. Jakubovics, *Nat. Rev. Microbiol.*, 2010, **8**, 471–480.
6 M. Burmølle, T. R. Thomsen, M. Fazli, I. Dige, L. Christensen, P. Homøe, M. Tvede, B. Nyvad, T. Tolker-Nielsen, M. Givskov, C. Moser, K. Kirketerp-Møller, H. K. Johansen, N. Høiby, P. Ø. Jensen, S. J. Sørensen and T. Bjarnsholt, *FEMS Immunol Med Microbiol*, 2010, **59**, 324–336.
7 J. G. Camp, M. Kanther, I. Semova and J. F. Rawls, *Gastroenterology*, 2009, **136**, 1989–2002.
8 P. D. Marsh, *Adv. Dent. Res.*, 1994, **8**, 263–271.
9 S. Macfarlane and J. F. Dillon, *J. Appl. Microbiol.*, 2007, **102**, 1187–1196.
10 M. J. Federle and B. L. Bassler, *J. Clin. Invest.*, 2003, **112**, 1291–1299.
11 C. Fuqua and E. P. Greenberg, *Nat. Rev. Mol. Cell Biol.*, 2002, **3**, 685–695.
12 J. Lee, A. Jayaraman and T. K. Wood, *BMC Microbiol.*, 2007, **7**, 42.
13 M. J. Kirisits and M. R. Parsek, *Cell. Microbiol.*, 2006, **8**, 1841–1849.
14 M. Hentzer, L. Eberl, J. Nielsen and M. Givskov, *BioDrugs*, 2003, **17**, 241–250.
15 G. W. Tannock, *Appl. Env. Microbiol.*, 1977, **33**, 745–750.
16 T. Smith, *J. Exp. Med.*, 1897, **2**, 543–547.
17 T. Bansal, D. Englert, J. Lee, M. Hegde, T. K. Wood and A. Jayaraman, *Infect. Immun.*, 2007, **75**, 4597–4607.
18 J. Domka, J. Lee and T. K. Wood, *Appl. Environ. Microbiol.*, 2006, **72**, 2449–2459.
19 D. A. Karlin, A. J. Mastromarino, R. D. Jones, J. R. Stroehlein and O. Lorentz, *J. Cancer Res. Clin. Oncol.*, 1985, **109**, 135–141.
20 E. Zuccato, M. Venturi, G. Di Leo, L. Colombo, C. Bertolo, S. B. Doldi and E. Mussini, *Dig. Dis. Sci.*, 1993, **38**, 514–519.
21 L. Rui, K. F. Reardon and T. K. Wood, *Appl. Microbiol. Biotechnol.*, 2005, **66**, 422–429.
22 B. D. Ensley, B. J. Ratzkin, T. D. Osslund, M. J. Simon, L. P. Wackett and D. T. Gibson, *Science*, 1983, **222**, 167–169.
23 A. Fishman, Y. Tao, L. Rui and T. K. Wood, *J. Biol. Chem.*, 2005, **280**, 506–514.
24 Y. Tao, A. Fishman, W. E. Bentley and T. K. Wood, *J. Bacteriol.*, 2004, **186**, 4705–4713.
25 J. Lee, T. Bansal, A. Jayaraman, W. E. Bentley and T. K. Wood, *Appl. Environ. Microbiol.*, 2007, **73**, 4100–4109.
26 J. Lee, C. Attila, S. L. Cirillo, J. D. Cirillo and T. K. Wood, *Microb. Biotechnol.*, 2009, **2**, 75–90.
27 C. Sternberg and T. Tolker-Nielsen, in *Current Protocols in Microbiology*, John Wiley & Sons, Inc., 2005.
28 M. R. Benoit, C. G. Conant, C. Ionescu-Zanetti, M. Schwartz and A. Matin, *Appl. Environ. Microbiol.*, 2010, **76**, 4136–4142.
29 H. Cho, H. Jönsson, K. Campbell, P. Melke, J. W. Williams, B. Jedynak, A. M. Stevens, A. Groisman and A. Levchenko, *PLoS Biol.*, 2007, **5**, 302–308.
30 K. P. Kim, Y.-G. Kim, C.-H. Choi, H.-E. Kim, S.-H. Lee, W.-S. Chang and C.-S. Lee, *Lab Chip*, 2010, **10**, 3296–3299.
31 J.-H. Lee, J. Kaplan and W. Lee, *Biomed. Microdevices*, 2008, **10**, 489–498.
32 K. A. Datsenko and B. L. Wanner, *Proc. Natl. Acad. Sci. U. S. A.*, 2000, **97**, 6640–6645.
33 M. C. Hansen, R. J. Palmer, Jr., C. Udsen, D. C. White and S. Molin, *Microbiol.*, 2001, **147**, 1383–1391.
34 R. D. Snaith, *Biochem. Educ.*, 1984, **12**, 187–187.
35 J. Kim, M. Hegde and A. Jayaraman, *Lab Chip*, 2010, **10**, 43–50.
36 A. Heydorn, A. T. Nielsen, M. Hentzer, C. Sternberg, M. Givskov, B. K. Ersbøll and S. Molin, *Microbiol.*, 2000, **146**, 2395–2407.
37 S. K. W. Dertinger, D. T. Chiu, N. L. Jeon and G. M. Whitesides, *Anal. Chem.*, 2001, **73**, 1240–1246.
38 D. L. Englert, M. D. Manson and A. Jayaraman, *Nat. Protoc.*, 2010, **5**, 864–872.
39 M. W. Toepke and D. J. Beebe, *Lab Chip*, 2006, **6**, 1484–1486.
40 G. Jagura-Burdzy and D. Hulanicka, *J. Bacteriol.*, 1981, **147**, 744–751.
41 A. F. González Barrios, R. Zuo, Y. Hashimoto, L. Yang, W. E. Bentley and T. K. Wood, *J. Bacteriol.*, 2006, **188**, 305–316.
42 J. W. Costerton, P. S. Stewart and E. P. Greenberg, *Science*, 1999, **284**, 1318–1322.